



Power generation from wind turbines in a solar chimney

Tudor Foote¹, Ramesh K. Agarwal²

¹ Graduate Student, Department of Mechanical Engineering & Materials Science, Washington University in St. Louis, Jolley Hall, Campus Box 1185, One Brookings Drive, St. Louis, Missouri, 63130, USA.

² William Palm Professor, Department of Mechanical Engineering & Materials Science, Washington University in St. Louis, Jolley Hall, Campus Box 1185, One Brookings Drive, St. Louis, Missouri, 63130, USA.

Abstract

Recent studies have shown that shrouded wind turbines can generate greater power compared to bare turbines. A solar chimney generates an upward draft of wind inside a tower and a shroud around the wind turbine. There are numerous empty silos on farms in the U.S. that can be converted to solar chimneys with minor modifications at modest cost. The objective of this study is to determine the potential of these silos/chimneys for generating wind power. The study is conducted through analytical/computational approach by employing the commercial Computational Fluid Dynamics (CFD) software. Computations are performed for five different geometric configurations consisting of a turbine, a cylindrical silo, and/or a venturi and/or a diffuser using the dimensions of typical silos and assuming Class 3 wind velocity. The incompressible Navier-Stokes equations with the Boussinesq approximation and a two equation realizable $k - \epsilon$ model are employed in the calculations, and the turbine is modeled as an actuator disk. The power coefficient (C_p) and generated power are calculated for the five cases. Consistent with recent literature, it was found that the silos with diffusers increase the C_p beyond Betz's limit significantly and thus the generated power. It should be noted that C_p is calculated by normalizing it by the turbine area swept by the wind. This study shows the potential of using abandoned silos in the mid-west and other parts of the country for localized wind power generation.

Copyright © 2013 International Energy and Environment Foundation - All rights reserved.

Keywords: Small wind turbines; Shrouded turbines; Betz's limit; Solar chimney.

1. Introduction

In past several years, several studies have shown that the shrouded wind turbines can generate greater power compared to bare turbines. A solar chimney not only generates an upward draft of the wind inside the solar tower but also creates a shroud around the wind turbine. There is large number of empty silos on farms, especially in mid-western U.S. The objective of this study is to determine the potential of these silos for generating wind-power with a wind turbine inside the silo. Figure 1 shows a typical silo enclosed by the staves (blocks). A typical silo is 70 ft. in height and 15 – 18 ft. in outside diameter. The dimensions of a stave or block are 10 inch horizontal x 30 inch vertical x 3.5 inch thick. The staves are offset vertically by 6 inch as shown in Figure 1. These staves can be removed from various locations around the periphery of the silo and can serve as inlets for the outside air. The air sucked-in through these inlets will move upward through the silo (like in a chimney) due to temperature differential between the lower and upper part of the silo (the air at lower part of the silo being at higher temperature).

At the top, the silo will be open to the outside atmosphere. A wind turbine can be installed inside the silo at a suitable height from the ground to extract the kinetic energy of the wind flowing upward from the inlets due to natural convection. The potential of this concept for wind power generation is evaluated by numerical simulation.

An analytical/computational study is performed to evaluate this potential by employing the well known commercial Computational Fluid Dynamics (CFD) software FLUENT [1]. An actuator disc model is used to model the turbine [2-5]. The incompressible Navier-Stokes equations with Boussinesq approximation and a two equation realizable $k - \epsilon$ model are employed in the calculations. C_p and generated power are calculated. It is found that the silo increases the C_p beyond the Betz's limit significantly and as a result the generated power; this effect is consistent with that found in the recent literature for shrouded wind turbines [6, 7]. It is important to note that C_p is calculated by normalizing it by the turbine area swept by the wind.

The study in this paper shows that the existing silos on the farms can be utilized for generating power from the wind by installation of wind turbines inside them. Although a simple model (actuator disc model) of a wind turbine has been employed in the CFD study, the estimates of C_p and generated wind power are reasonably accurate and can be used to assess the economic feasibility of this idea for energy generation.



Figure 1. A typical silo on a farm

2. Technical approach

The performance of a wind turbine inside a vertical silo is modeled by creating an actuator disc model in the commercial CFD solver FLUENT. The geometries of the three configurations studied are shown in Figures 2(a) - 2(c). In Figure 2(a), the silo is modeled as a circular cylinder with the top open to the atmosphere. In Figure 2(b), a venturi (a converging – diverging nozzle) is created around the turbine inside the silo. In Figure 2(c), a diverging diffuser section is placed on top of the silo; this section need

not be made of staves and can be of a light weight structurally strong material to withstand the forces due to class – 3 winds. Various parameters shown in Figure 2 can be easily varied in the computer program to determine their effect on wind power generation.

The geometric models of Figure 2 are created in the software “GAMBIT” [8]. A structured mesh is generated in the axi-symmetric models which is clustered near the actuator disc and near the silo walls. Computations are performed on two set of grids – coarse and fine in order to ensure the grid independence of the solution. The incompressible Navier-Stokes equations with the Boussinesq approximation and a two equation realizable $k - \epsilon$ model are employed in the CFD solver for all calculations.

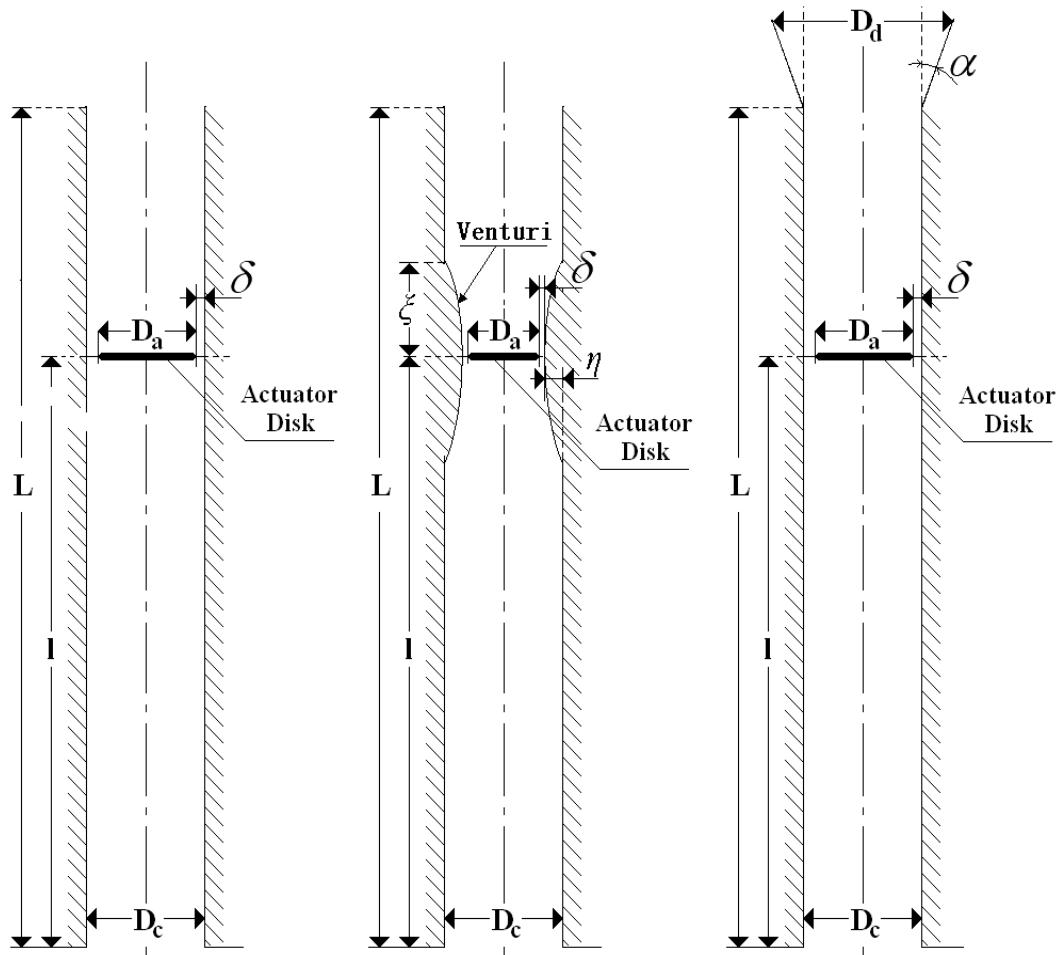


Figure 2. (a) Computational geometry of a cylindrical silo (without diffuser), (b) Computational geometry of a cylindrical silo with a venturi around the turbine, (c) Computational geometry of a cylindrical silo with diffuser on the top; L = height of the silo, D_c = interior diameter of the cylindrical silo, D_a = diameter of the turbine modeled as an actuator disc, l = height of the turbine from the ground, δ = clearance between the turbine and the silo wall, D_d = diameter of the exit section of the diffuser, α = diffuser angle, ξ and η define the parameters related to venturi.

3. Results

As mentioned before in the “Introduction” section, first the mathematical model (actuator disc) was validated by computing the power coefficient (C_p) for a bare-turbine; a C_p value close to Betz’s limit (~ 0.59) was obtained. In the validation, the flow was assumed to be inviscid, incompressible and irrotational (potential flow). After the validation, calculations were performed for five cases using the dimensions of two typical silos of different diameters geometrically modeled as shown in Figure 2 and assuming class - 3 wind velocity: (a) bare turbine (without enclosing silo), (b) turbine enclosed by a cylindrical silo, (c) the turbine enclosed by the cylindrical silo with a diffuser at the top of the silo, (d) turbine surrounded by a converging – diverging venturi inside a cylindrical silo, and (e) turbine

surrounded by a converging – diverging venturi inside a cylindrical silo with a diffuser at the top of the silo. The calculations for cases (b) – (e) were performed with a temperature differential between the ground and the top of the silo. C_p and generated power were calculated for the five cases. These results are described below for configurations 1-4.

It should be noted that the wind is sucked in through the openings created by removal of staves. We will call these openings ‘open-staves.’ Several effects can occur depending upon the placement of open-staves. If the open-staves are too close to the ground, the wind velocity will be significantly less than 5.6m/s. If they are approximately 4 -6 meters (15 – 20 ft.) above the ground, the wind velocity will be close to that in the atmosphere for that particular day. However the wind will enter the silo nearly perpendicular to the cylindrical surface. As it moves upward in the silo, it creates a region of separation near the entrance of the open-staves. We studied this effect by assuming a cylindrical opening of 30 inch height at a distance of 5 meters (16 ft.) above the ground. It turns out that within a distance of less than 1 meter (~ 3 ft.), the flow becomes attached again. Therefore, assuming a wind of velocity V facing the turbine at a height of 50 ft from the ground is a reasonable and good approximation for the calculations.

The wind velocity in a vertical silo is also a function of the temperature differential between the ground and top of the silo. Since the silo height is only 70 ft, this temperature differential ΔT is very small; it is 0.025deg F (based on 0.00357deg.F /ft). The buoyancy effect on the upward flowing air in increasing its speed is therefore very small. This effect can be increased by increasing the temperature of the sucked-in air near the ground by some means such as electric heaters appropriately placed or by placing solar panels near the ground (it creates a solar chimney configuration). The effect of increasing ΔT on increasing the upward wind velocity and therefore the turbine power is also calculated.

Configuration 1A (Figure 2(a)): $L = 70$ ft, $l = 50$ ft, $D_c = 11$ ft, $D_a = 10$ ft, $\delta = 0.5$ ft, $\Delta T = 0, 2, 4, 6,$ and 8 deg. The wind velocity of class 3 wind was assumed to be $V = 5.6$ m/s facing normal to the actuator disc (turbine).

Configuration 1B (Figure 2(a)): $L = 70$ ft, $l = 50$ ft, $D_c = 17.6$ ft, $D_a = 16$ ft, $\delta = 0.8$ ft, $\Delta T = 0, 2, 4, 6,$ and 8 deg. The wind velocity of class 3 wind was assumed to be $V = 5.6$ m/s facing normal to the actuator disc (turbine).

The difference between configuration 1A and 1B is in the diameters of the two silos D_c and diameters of the turbines D_a . Table 1 provides the power generated by the turbine, the power available in the turbine swept area of the wind, and the turbine efficiency for the cylindrical silo geometry of configuration 1A (Figure 2(a)) and class -3 wind speed of 5.6m/s for various values of ΔT .

Table 1. Power generated by the turbine in cylindrical silo (Configuration 1A) of Figure 2(a) and turbine efficiency

ΔT [°C]	Power [W]	Wind Energy [W]	C_p
0	290	785	0.37
2	328	785	0.42
4	367	785	0.47
6	408	785	0.52

From Table 1, it can be seen that the increase in ΔT increases the generated power as well as the turbine efficiency.

Figure 3 shows the entire computational domain employed for the case of the turbine inside the cylindrical silo. Figure 3(a) shows the velocity magnitude contours of the flow for $\Delta T = 0$. Figure 3(b) shows the static pressure contours in field (in Pascals) for $\Delta T = 0$.

Figure 3(b) shows that most of the pressure variation is confined to the region near the actuator disc; the pressure upstream of the disc is greater than that on downstream side as expected. Velocity and pressure contours similar to Figures 3(a) and 3(b) are obtained for other values of ΔT with minor changes.

Table 2 provides the power generated by the turbine and the turbine efficiency for the cylindrical silo geometry of configuration 1B (Figure 2(a)) and class -3 wind speed of 5.6m/s for various values of ΔT .

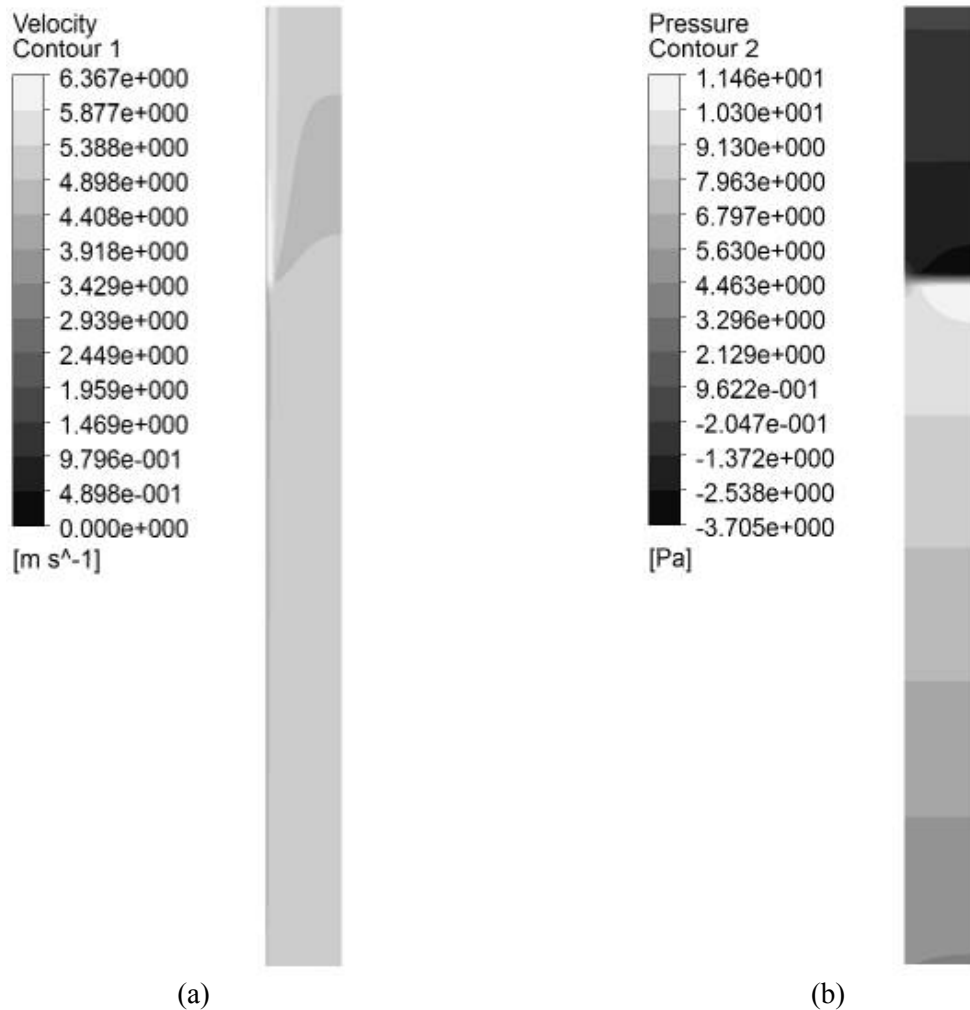


Figure 3. Axisymmetric computational domain for flow inside the silo enclosing the turbine; Configuration 1A, $\Delta T = 0$: (a) Velocity magnitude contours, (b) Static pressure magnitude contours

Table 2. Power generated by the turbine in cylindrical silo (Configuration 1B) of Figure 2(a) and turbine efficiency

ΔT [$^{\circ}\text{C}$]	Power [W]	Wind Energy [W]	C_p
0	748	2016	0.37
2	907	2016	0.45
4	1075	2016	0.53
6	1253	2016	0.62
8	1439	2016	0.72

From Table 2, it can be seen that larger diameter silo and turbine generate greater wind power as expected. Also, like before for configuration 1A, the increase in ΔT increases the generated power as well as the turbine efficiency. However, there is little difference in the turbine efficiency between configuration 1A and configuration 1B as expected. Figures analogous to Figures 3(a) and 3(b) are not presented for this configuration because they are qualitatively similar in flow pattern and contours.

Configuration 2A (Figure 2(c)): $L = 70$ ft, $l = 50$ ft, $D_c = 11$ ft, $D_a = 10$ ft, $\delta = 0.5$ ft, $\alpha = 20$ deg, $D_d = 1.5 \times D_c$, $\Delta T = 0, 2, 4, 6,$ and 8 deg. The wind velocity of class 3 wind was assumed to be $V = 5.6$ m/s facing normal to the actuator disc (turbine).

Configuration 2B (Figure 2(c)): $L = 70$ ft, $l = 50$ ft, $D_c = 17.6$ ft, $D_a = 16$ ft, $\delta = 0.8$ ft, $\alpha = 20$ deg, $D_d = 1.5 \times D_c$, $\Delta T = 0, 2, 4, 6,$ and 8 deg. The wind velocity of class 3 wind was assumed to be $V = 5.6$ m/s facing normal to the actuator disc (turbine).

Table 3 provides the power generated by the turbine and the turbine efficiency for the cylindrical silo geometry (configuration 2A) with a diffuser on the top (Figure 2(c)) and class -3 wind speed of 5.6m/s for various values of ΔT .

Table 3. Power generated by the turbine in cylindrical silo (Configuration 2A) with a diffuser at top (Figure 2(c)) and turbine efficiency

ΔT [°C]	Power [W]	Wind Energy [W]	Cp
0	560	785.00	0.71
2	642	785.00	0.82
4	727	785.00	0.93
6	816	785.00	1.04
8	909	785.00	1.16

From Table 3, it can be seen that the diffuser on the top has a significant effect in increasing the turbine power as well as the turbine efficiency which further increases with increase in ΔT .

Figure 4 shows the zoomed-in view of the computational domain near the actuator disc employed for the case of the turbine inside the cylindrical silo with a diffuser on the top. Figure 4(a) shows the velocity magnitude of the flow for $\Delta T = 6$. Figure 4(b) shows the zoomed-in-view of static pressure contours in field (in Pascals) for $\Delta T = 6$.

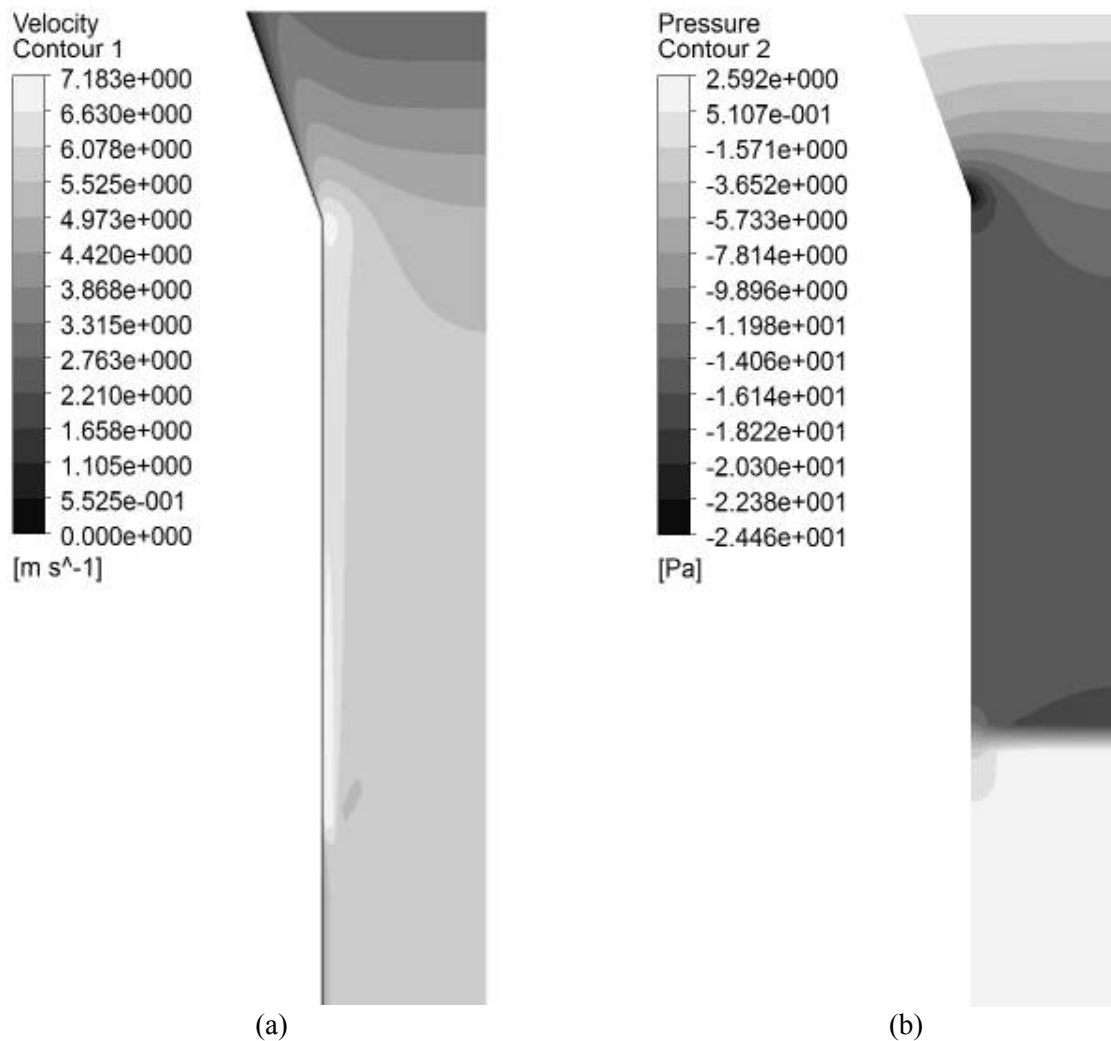


Figure 4. Zoomed-in-view of computational domain for flow inside the silo enclosing the turbine with a diffuser on the top; Configuration 2A, $\Delta T = 6$: (a) Velocity magnitude contours, (b) Static pressure magnitude contours

Table 4 provides the power generated by the turbine and the turbine efficiency for the cylindrical silo geometry (configuration 2B) with a diffuser on the top (Figure 2(c)) and class -3 wind speed of 5.6m/s for various values of ΔT .

Table 4. Power generated by the turbine in cylindrical silo (Configuration 2B) with a diffuser at top (Figure 2(c)) and turbine efficiency

ΔT [°C]	Power [W]	Wind Energy [W]	Cp
0	1463	2016	0.73
2	1815	2016	0.90
4	2176	2016	1.08
6	2580	2016	1.28
8	2984	2016	1.48

From Table 4, it can be seen that the diffuser on the top has a significant effect in increasing the turbine power as well as the turbine efficiency which further increases with increase in ΔT . Also, it can be seen that larger diameter silo and turbine generate greater wind power as expected. Furthermore, like before for configuration 2A, the increase in ΔT increases the generated power as well as the turbine efficiency. Figures analogous to Figure 4 are not presented for this configuration because they are qualitatively similar in flow pattern and contours.

Configuration 3A (Figure 2(b)): $L = 70$ ft, $l = 50$ ft, $D_c = 11$ ft, $D_a = 8$ ft, $\xi = 4$ ft., $\eta = 1.1$ ft., $\delta = 0.4$ ft, $\Delta T = 0, 2, 4,$ and 6 deg. This configuration is similar to the configuration in Figure 2(a) with a venturi surrounding the turbine.

Configuration 3B (Figure 2(b)): $L = 70$ ft, $l = 50$ ft, $D_c = 17.6$ ft, $D_a = 12.8$ ft, $\xi = 4$ ft., $\eta = 1.76$ ft., $\delta = 0.64$ ft, $\Delta T = 0, 2, 4,$ and 6 deg. This configuration is similar to the configuration in Figure 2(a) with a venturi surrounding the turbine.

Table 5 provides the power generated by the turbine and the turbine efficiency for the cylindrical silo geometry (Configuration 3A) with a converging-diverging venturi (Figure 2(b)) and class -3 wind speed of 5.6m/s for various values of ΔT .

Table 5. Power generated by the turbine in a cylindrical silo (Configuration 3A) with a venturi surrounding it (Figure 2(b)) and turbine efficiency

ΔT [°C]	Power [W]	Wind Energy [W]	Cp
0	297	502	0.59
2	336	502	0.67
4	376	502	0.75
6	418	502	0.83
8	462	502	0.92

In Table 5, it should be noted that the available wind power in this case is less compared to that in Tables 1 and 2 because the wind turbine diameter in this case is $D_a = 8$ ft. compared to that in configurations 1A and 2A where the wind turbine diameter $D_a = 10$ ft. The diameter of the turbine had to be less in this case because of the installation of the venturi. Nevertheless, Table 5 shows that the venturi surrounding the turbine (even for a smaller turbine) has a significant effect in increasing the turbine power as well as the turbine efficiency which further increases with increase in ΔT .

Figure 5 shows the zoomed-in view of the computational domain near the actuator disc employed for the case of the turbine surrounded by a converging – diverging venturi inside the cylindrical silo. Figure 5(a) shows the velocity contours indicating the magnitude of the flow for $\Delta T = 6$. Figure 5(b) shows the zoomed-in-view of static pressure contours in the field (in Pascals) for $\Delta T = 6$.

Table 6 provides the power generated by the turbine and the turbine efficiency for the cylindrical silo geometry (Configuration 3B) (Figure 2(b)) and class -3 wind speed of 5.6m/s for various values of ΔT .

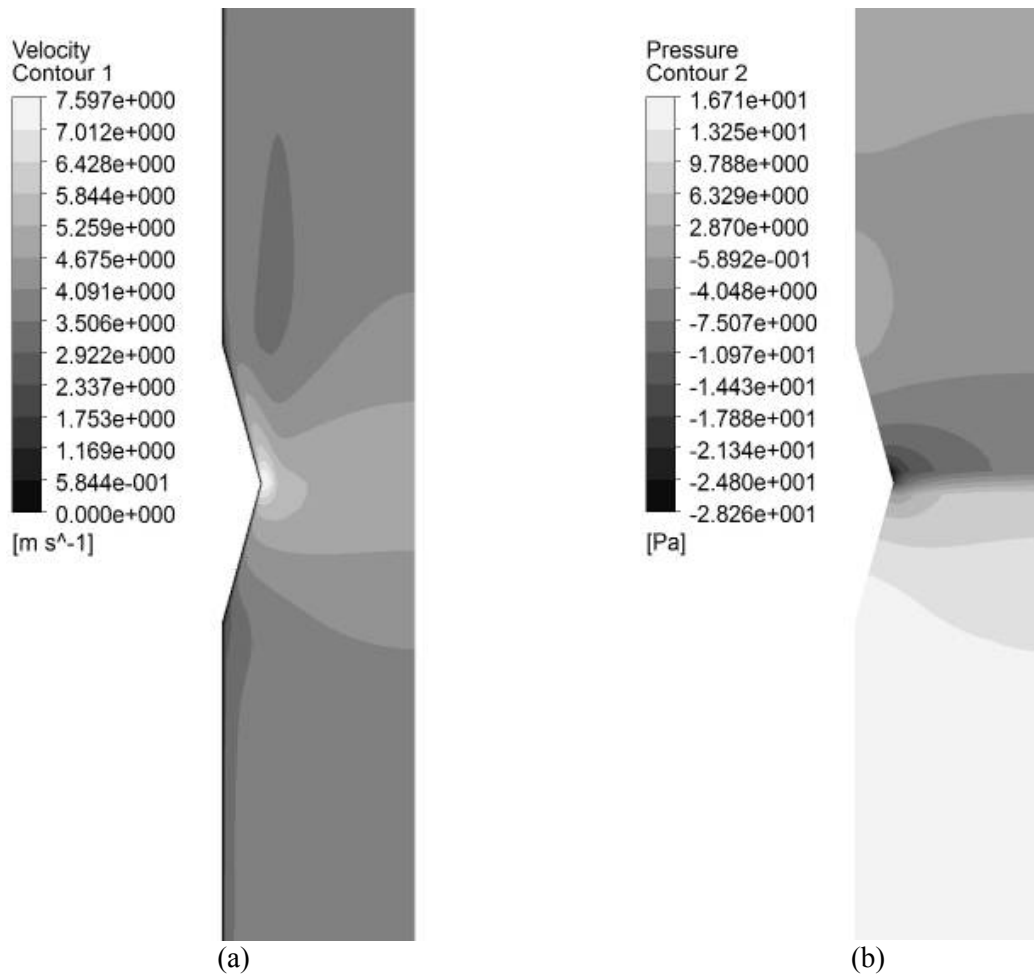


Figure 5. Zoomed-in-view of computational domain for flow inside the silo with a turbine surrounded by the venturi (Configuration 3A) (Figure 2(b)); $\Delta T = 6$: (a) Velocity magnitude contours, (b) Static pressure contours.

Table 6. Power generated by the turbine in a cylindrical silo (Configuration 3A) with a venturi Surrounding it (Figure 2(b)) and turbine efficiency

ΔT [$^{\circ}\text{C}$]	Power [W]	Wind Energy [W]	C_p
0	768	1285	0.60
2	931	1285	0.72
4	1104	1285	0.86
6	1286	1285	1.00
8	1478	1285	1.15

From Table 6, it can be seen that the converging-diverging venturi surrounding the turbine has a significant effect in increasing the turbine power as well as the turbine efficiency which further increases with increase in ΔT . Also, it can be seen that larger diameter silo and turbine generate greater wind power as expected. Furthermore, like before for configuration 3A, the increase in ΔT increases the generated power as well as the turbine efficiency. Figures analogous to Figure 5 are not presented for this configuration because they are qualitatively similar in flow pattern and contours.

Configuration 4A (Figure 2(b) with a Diffuser on the top): $L = 70$ ft, $l = 50$ ft, $D_c = 11$ ft, $D_a = 8$ ft, $\xi = 4$ ft., $\eta = 1.1$ ft., $\delta = 0.4$ ft, $\alpha = 20$ deg, $D_d = 1.5 D_c$, $\Delta T = 0, 2, 4,$ and 6 deg. This configuration is similar to the configuration 3 with a diffuser on the top.

Configuration 4B (Figure 2(b) with a Diffuser on the top): $L = 70$ ft, $l = 50$ ft, $D_c = 17.6$ ft, $D_a = 12.8$ ft, $\xi = 4$ ft., $\eta = 1.76$ ft., $\delta = 0.64$ ft, $\alpha = 20$ deg, $D_d = 1.5 D_c$, $\Delta T = 0, 2, 4,$ and 6 deg. This configuration is similar to configuration 3 with a diffuser on the top.

Table 7 provides the power generated by the turbine and the turbine efficiency for the cylindrical silo geometry with a converging-diverging venturi (Figure 2(b)) surrounding the turbine and a diffuser at the top of the silo (configuration 4A), and class -3 wind speed of 5.6m/s for various values of ΔT .

Table 7. Power generated by the turbine in cylindrical silo with a venturi surrounding it (Figure 2(b)) and a diffuser at the top of the silo (Configuration 4A) and turbine efficiency

ΔT [°C]	Power [W]	Wind Energy [W]	Cp
0	422	502	0.84
2	483	502	0.96
4	548	502	1.09
6	615	502	1.22
8	684	502	1.36

In Table 7, it should be noted that similar to Table 5, the available wind power in this case is less compared to that in Tables 1 and 3 because the wind turbine diameter in this case is $D_a=8$ ft. compared to that in configurations 1A and 2A where the wind turbine diameter $D_a=10$ ft. The diameter of the turbine had to be less in this case because of the installation of the venturi. Nevertheless, Table 7 shows that diffuser at the top of the silo has a significant effect in increasing the turbine power as well as the turbine efficiency (compare the results with those in Table 5), which further increases with increase in ΔT .

Figure 6 shows the zoomed-in view of the computational domain near the actuator disc employed for the case of the turbine surrounded by a converging – diverging venturi inside the cylindrical silo with a diffuser on the top. Figure 6(a) shows the velocity magnitude contours of the flow for $\Delta T = 6$. Figure 6(b) shows the zoomed-in-view of static pressure contours in field (in Pascals) for $\Delta T = 6$.

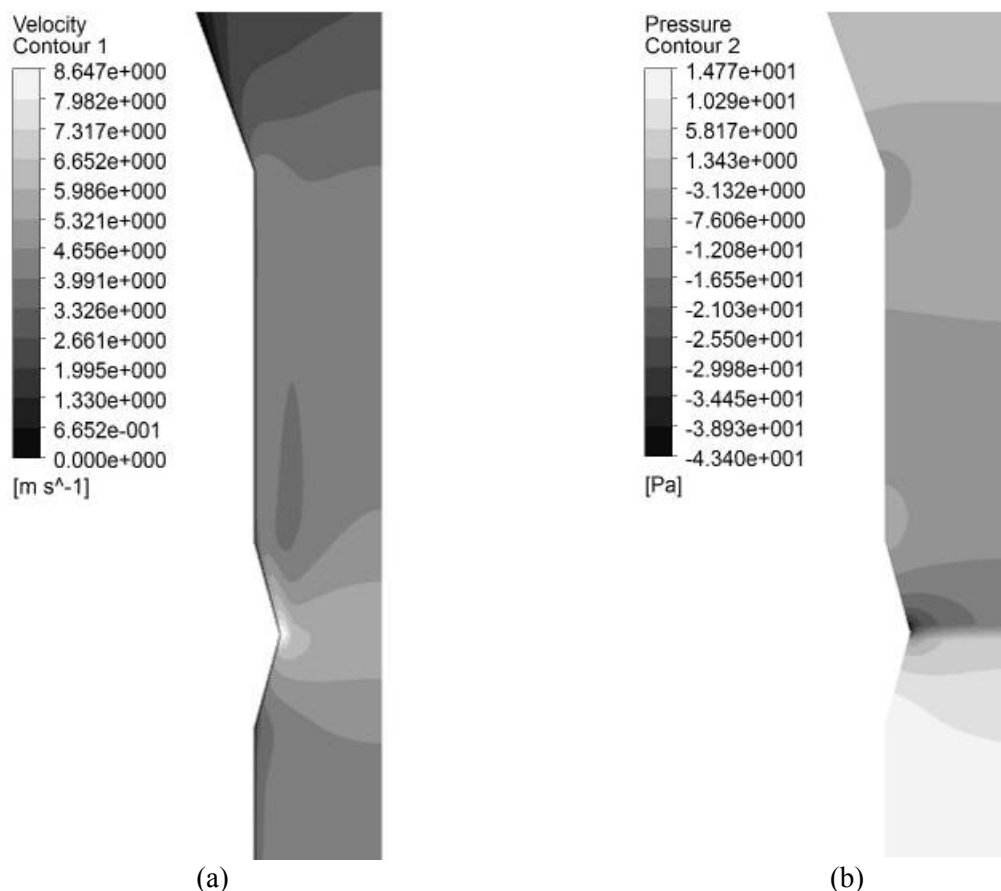


Figure 6. Zoomed-in-view of computational domain for flow inside the silo with a turbine surrounded by the venturi and a diffuser on the top; $\Delta T = 6$: (a) Velocity magnitude contours, (b) Static pressure contours.

Table 8 provides the power generated by the turbine and the turbine efficiency for the cylindrical silo geometry with a converging-diverging venturi (Figure 2(b)) surrounding the turbine and a diffuser at the top of the silo (configuration 4B), and class -3 wind speed of 5.6m/s for various values of ΔT .

Table 8. Power generated by the turbine in a cylindrical silo with a venturi surrounding it (Figure 2(b)) and a diffuser at the top of the silo (Configuration 4B) and turbine efficiency

ΔT [°C]	Power [W]	Wind Energy [W]	C_p
0	1108	1285	0.86
2	1369	1285	1.06
4	1649	1285	1.28
6	1946	1285	1.51
8	2260	1285	1.76

In Table 8, it should be noted that similar to Table 6, the available wind power in this case is less compared to that in Tables 2 and 4 because the wind turbine diameter in this case is $D_a = 12.8$ ft. compared to that in configurations 1B and 2B where the wind turbine diameter $D_a = 16$ ft. The diameter of the turbine had to be less in this case because of the installation of the venturi. Nevertheless, Table 8 shows that diffuser at the top of the silo has a significant effect in increasing the turbine power as well as the turbine efficiency (compare the results with those in Table 6), which further increases with increase in ΔT . Figures analogous to Figure 6 are not presented for this configuration because they are qualitatively similar in flow pattern and contours.

4. Discussions and conclusions

The results of this study show that the existing silos on the farms can be utilized for generating power from the wind by installation of wind turbines inside them. The power from 1kW (for a silo ~ 12 ft. diameter) to 2 kW (for a silo of ~ 18 ft. diameter) can be obtained from class 3 winds of velocity ~ 6m/s. Efficiency of wind power generation can be increased by creating a temperature difference between the ground and top of the silo and by surrounding the turbine by a converging-diverging venturi. However, the addition of a diffuser section on the top of the silo appears to be the most efficient, simple as well as economical way of significantly increasing the power generation from a wind turbine. The silos are more efficient in wind power generation than the bare horizontal axis turbines because of shrouding effects which allow the efficiency to exceed the ideal Betz's limit. Although a simple model (actuator disc model) of a wind turbine has been employed in this CFD study, the estimates of C_p and generated wind power are reasonably accurate and can be used to assess the economic feasibility of this idea for energy generation. Although the results reported here are for two typical silo dimensions and class 3 wind speed, they can be rapidly generated for other geometries and wind speeds since the basic formulation and its implementation in the CFD solver have been accomplished.

5. Future work

There are many issues that require further investigation: (a) *the proper placement of stave-openings to draw wind inside the silo*: If the stave-openings are very close to the ground, the wind velocity becomes very small because of the atmospheric boundary layer. Even if the stave-openings are at a reasonably higher level from the ground, their placement at a proper distance from the turbine is critical since the wind stream will separate away from the walls of the silo near the entrance of the stave-openings; (b) *the increase in the updraft velocity of the wind because of temperature stratification*: For an average height of about 70ft, the temperature differential ΔT between the bottom and top of the silo is very small; it is 0.025deg F (based on 0.00357deg.F/ft). It is not enough to create any significant updraft and increase in wind velocity. The only way to increase the wind velocity upward is to provide heat at the lower level near the stave-openings. The calculations show that that larger ΔT increases the wind velocity and therefore the turbine power. However, the energy needed for heating the ground level air for a desired value of ΔT should be estimated and compared with the additional energy generated by the wind turbine (due to increase in wind speed) in order to determine the benefit of ground level heating, (c) *the venturi shape* (the axial length and boundary shape) should be optimized by using an optimization algorithm (e.g. a genetic algorithm) to extract maximum power from the wind, (d) *the diffuser shape* (the axial length and boundary shape) should be optimized by using an optimization algorithm (e.g. a genetic algorithm) to extract

additional power from the wind, and (e) *the full scale 3D CFD simulations* should be performed by including the knowledge from items (a) – (d) for a 3-bladed rotor with optimized blade designs for various blade tip to wind speed ratios ($\lambda = \Omega D/2V$, where Ω = rotational speed of the rotor, D is the rotor diameter and V is the wind velocity facing the rotor). Addressing these five issues will help in determining the best possible configuration for generating maximum wind power from wind turbines enclosed by silos. Once this configuration is determined, the cost estimates for initial investment and return on investment (ROI) should be conducted taking into account the number of such installations. The installation and maintenance issues should also be addressed.

References

- [1] FLUENT 6.3: Flow Modeling Software, Ansys Inc., 2007.
- [2] Mikkelsen, R., "Actuator Disc Methods applied to Wind Turbines," PhD thesis, Technical University of Denmark, Copenhagen, June 2003.
- [3] Manwell, J.F., McGowan, J.G. and Rogers, A.L., Wind Energy Explained, John Wiley, 2nd edition, 2009.
- [4] Hansen, M.O.L., Aerodynamics of Wind Turbines, Earthscan, Sterling, VA, 2000.
- [5] Burton, T., Sharped, D., Jenkins, N. and Bossanyi, E., Wind Energy Hand Book, John Wiley, 2001.
- [6] Hansen, M.O.L., Sorenson, N.N., Flay, R.G.J., "Effect of Placing a Diffuser around a Wind Turbine," Wind Engineering, Vol. 3, No. 4, 2000, pp. 207-213.
- [7] Werle, M.J. and Presz, Jr., W.M., "Shroud and Ejector Augmenters for Subsonic Propulsion," AIAA J. of Propulsion and Power, Vol. 25, No. 1, 2009, pp. 228-236.
- [8] GAMBIT 6.2: Geometry and Mesh Generation Preprocessor, Ansys Inc., 2007.



Tudor Foote graduated with a M.S in Mechanical Engineering in December 2011 from the Department of Mechanical Engineering & Materials Science at Washington University in St Louis. He received B.S. in Mechanical Engineering also from Washington University. Tudor's research focuses on wind energy and aerodynamics. He is currently working on shape optimizations for shrouds for small horizontal-axis wind turbines (HAWT) using CFD method and genetic algorithms.
E-mail address: tffoote@gmail.com



Ramesh K. Agarwal received the Ph.D degree in aeronautical sciences from Stanford University, Palo Alto, CA, USA in 1975. His research interests are in the theory and applications of computational fluid dynamics to study the fluid flow problems in aerospace and renewable energy systems. He is currently the William Palm Professor of Engineering in department of Mechanical Engineering and Materials Science at Washington University in St. Louis, MO, USA. He is a Fellow of ASME, AIAA, IEEE, and SAE.
E-mail address: rka@wustl.edu

